Finite-amplitude compact wavepackets in rotating flows

Ted Johnson (UCL)

Nonlinear waves in Oceanography and Beyond
Roger Grimshaw @ 80
University of Southern Queensland
26th November 2018

Roger Hamilton James Grimshaw

Born 13/12/1938, in Auckland, New Zealand

- Primary: King's Preparatory School, Auckland, N.Z. (Dux, 1951)
- Secondary: King's College, Auckland, N.Z. (Dux, 1956)
- Tertiary: Auckland University, N.Z. (B.Sc., 1960, M.Sc. 1961, British Commonwealth Scholarship, 1961.)
- : Post-grad.: Cambridge University, U.K. (Ph.D., 1964, "Topics in the theory of wave propagation", supervised by Dr F.G. Friedlander, F.R.S.)

Roger Hamilton James Grimshaw

Post-doctoral career:

- Fulbright
  Travel grant, 1964, Courant Institute.
- 1965-1969 Snr.
  Lecturer, Dept of Maths, Univ of Melbourne
- 1970-1985
  Reader, Mathematics, Univ of Melbourne
- 1986-1992 Professor of Applied Mathematics, Univ of NSW
- 1992-1999, Professor of Applied Mathematics (Head from 1994-1997), Dept of Maths and Stats, Monash Univ;
- 2000-2013, Professor of Mathematical Sciences, Dept of Math Sciences, Loughborough Univ

Roger Hamilton James Grimshaw

Present Positions:

- Senior Research Associate, UCL
- Visiting Professor, Loughborough
- Visiting Professor, University of Exeter
- Adjunct Research Fellow, USQ

160 international meetings (invited speaker at 118)
335 refereed publications (148 since 2000)
7 books, 31 chapters in books, 38 conference proceedings.

- Elected Fellow of the Australian Academy of Sciences, 1990.
- Awarded the Centenary Medal of Australia, 2002
- Awarded the ANZIAM Medal, 2004.
- Elected Fellow of the Australasian Fluid Mechanics Society, 2012
- Elected Fellow of the Australian Mathematical Society, 2014

Finite-amplitude compact wavepackets in rotating flows

- Background and development
- The nonlinear IVP and the TNLS (energy transport from the zero-dispersion wavenumber in the GO equation)
- Results for strong rotation (small amplitude, NLS)
- Results for large amplitude (weak rotation, WMT)

Andaman Sea, SAR image

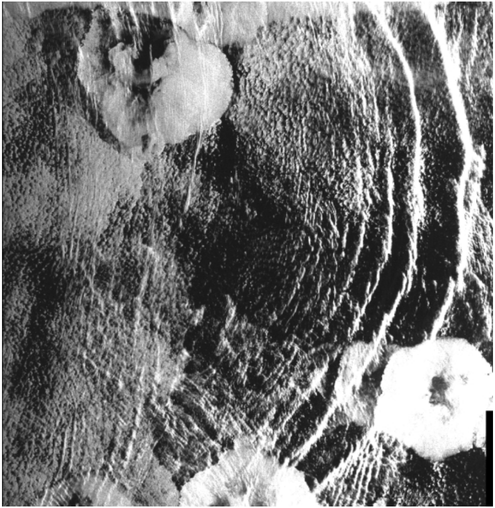

Surface signature of sub-surface interfacial solitary waves

Tang *et al.* 2014 *Sci. Rep.*

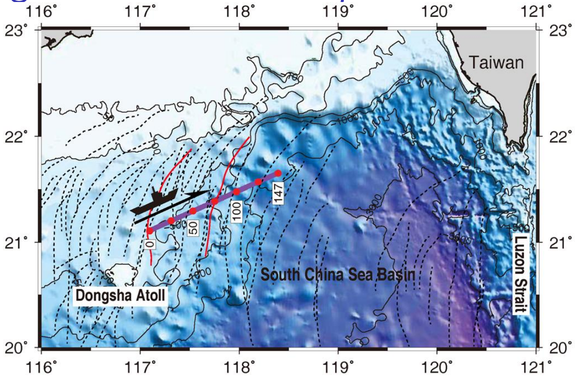

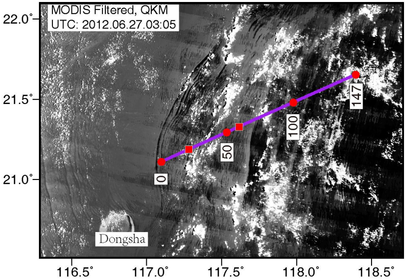

Tang *et al.* 2014 *Sci. Rep.*

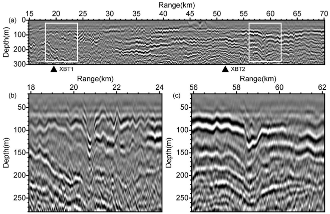

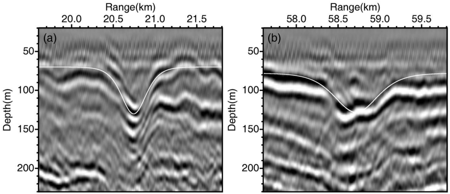

More recently, rotational effects:
Grimshaw, da Silva, and Magalhaes (2017) Modelling and observations oceanic nonlinear internal wave packets affected by the earth's rotation, *Ocean Modelling* **116**, 146-158.

The Ostrovsky equation

KdV with weak rotation:

$$\eta_t + \nu\eta\eta_x + \beta\eta_{xxx} = \gamma v, \qquad v_x = \eta.$$

ν nonlinearity; β non-hydrostatic; γ rotation

$$(\eta_t + \nu\eta\eta_x + \beta\eta_{xxx})_x = \gamma\eta.$$

Ostrovsky equation, (1978)

The scaled equation

- For the ocean $\nu\beta > 0$ and $\gamma > 0$.
- Write (Grimshaw & Helfrich, 2008), $x = L\tilde{x}$, $t = T\tilde{t}$, $\eta = M\tilde{\eta}$, where

$$L^4 = \beta/\gamma,\ T = L^3/\beta,\ M = \beta/\nu L^2$$

- Then

$$(\tilde{\eta}_t + \tilde{\eta}\tilde{\eta}_x + \tilde{\eta}_{xxx})_x = \tilde{\eta}.$$

  Parameter free. Drop tildes.
- The initial condition introduces a length scale and amplitude, A.

Linear waves

Neglect nonlinearity and look for solutions proportional to $\exp[\mathrm{i}(kx - \omega t)]$. Then

- $\omega = 1/k - k^3$,
- Phase speed, $c_p = -k^2 + 1/k^2$, (takes all values).
- Group velocity, $c_g = -3k^2 - 1/k^2$,
  (with maximum –negative– at $k_c = 3^{-1/4}$).

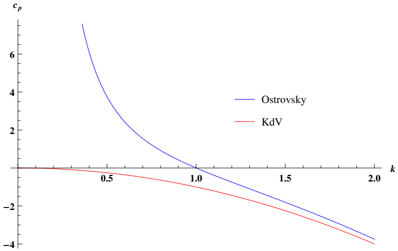

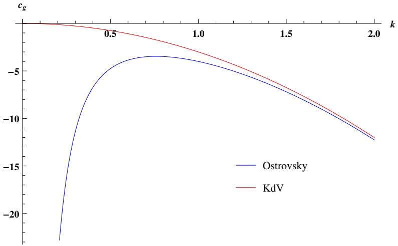

Large-amplitude (weak rotation)

For $A \gg 1$,

- Scale η on A, x on $A^{-1/2}$ and t on $A^{-3/2}$. Then
- $$(\eta_t + \eta\eta_x + \eta_{xxx})_x = \epsilon^2\eta,$$

  where $\epsilon = 1/A \ll 1$.
- Notice this is precisely the scaling for the KdV solitary wave. Near-KdV limit.
- KdV soliton with $c = 1$ is an exact solution when $\epsilon = 0$.

Terminal damping, $\epsilon \ll 1$

- Can show rigourously that there is no Wave of Translation once $\epsilon \neq 0$.
- Grimshaw, He, Ostrovsky (1998): Poincaré wave radiation destroys KdV soliton in time $A^{-1/2}/\epsilon^2$.
- In the parameter-free Ostrovsky equation this is simply t of order unity.

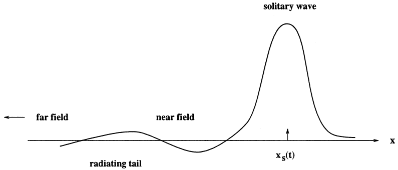

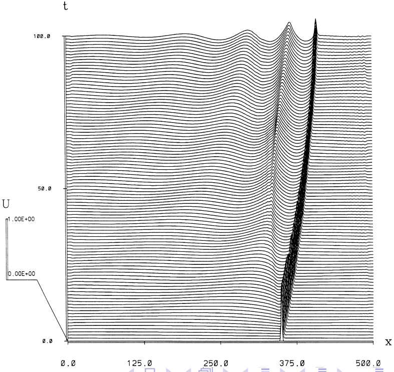

Terminal damping?

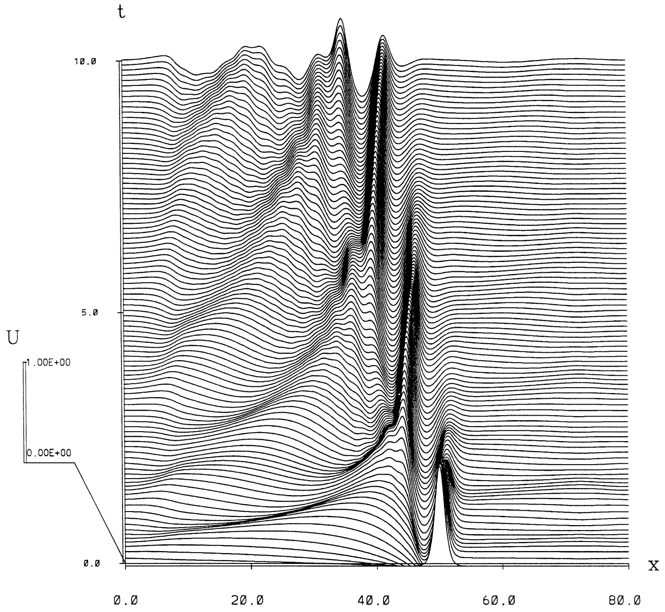

The answer

PHYSICS OF FLUIDS **19**, 026601 (2007)

Decay and return of internal solitary waves with rotation

Karl R. Helfrich[a)]
Department of Physical Oceanography, Woods Hole Oceanographic Institution, Woods Hole, Massachusetts 02543

(Received 22 September 2006; accepted 19 December 2006; published online 23 February 2007)

The effect of rotation on the propagation of internal solitary waves is examined. Wave evolution is followed using a new rotating extension of a fully nonlinear, weakly nonhydrostatic theory for waves in a two-layer system. When a solitary wave solution of the nonrotating equations is used as the initial condition, the wave initially decays by radiation of longer inertia-gravity waves. The radiated inertia-gravity wave always steepens, leading to the formation a secondary solitary-like wave. This decay and reemergence process then repeats. Eventually, a nearly localized wave packet emerges. It consists of a long-wave envelope and shorter, faster solitary-like waves that propagate through the envelope. The radiation from this mature state is very weak, leading to a robust, long-lived structure that may contain as much as 50% of the energy in the initial solitary wave. Interacting packets may either pass through one another, or merge to form a longer packet. The packets appear to be modulated, fully nonlinear versions of the steadily translating quasi-cnoidal waves. © *2007 American Institute of Physics*. [DOI: 10.1063/1.2472509]

MCC

Integrations of the Miyata-Choi-Camassa (MCC) (Helfrich 2007)

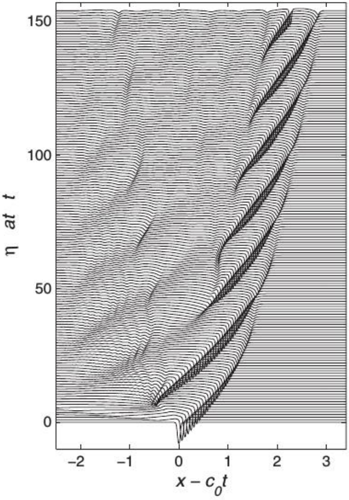

FIG. 1. Numerical solution for a solitary wave with $\eta_0 = -0.2$ and $[h_0, \beta^{1/2}] = [0.25, 0.02]$. The interface $\eta(x,t)$ is shown at equal time intervals in a frame moving with the linear wave speed c_0.

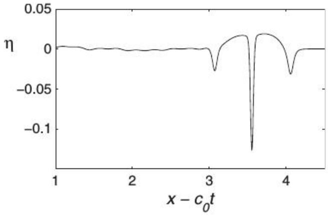

FIG. 4. The interface displacement of the leading wave packet from the run in Fig. 1 at $t=291.56$.

MCC

A nonlinear wavepacket (Helfrich 2007)

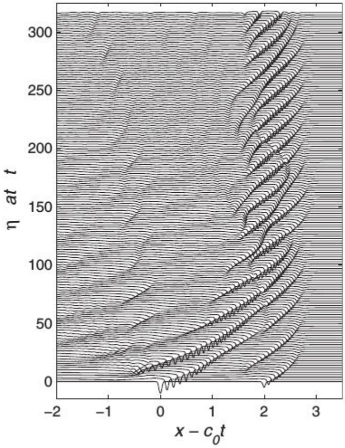

FIG. 9. Solution with two solitary waves, η_0=−0.2 and −0.1, and $[h_0, \beta^{1/2}]$=[0.25, 0.02]. The interface $\eta(x,t)$ is shown at equal time intervals in a frame moving with the linear wave speed c_0.

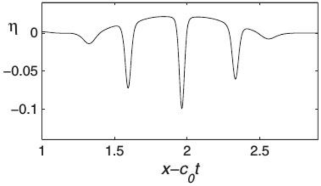

FIG. 10. The interface displacement of the leading wave packet from the run in Fig. 9 at t=415.69.

Wavepacket in a frame moving to the left at the speed of the envelope (WJ14)

Nonlinear wavepackets

Grimshaw & Helfrich (2008) - Ostrovsky equation

- Wavepackets travel at speeds very close to $c_g(k_c)$, the maximum of the group velocity (negative i.e. less than linear longwave speed)
- Weakly nonlinear, prototypical equation: Nonlinear Schrödinger equation (NLS).
- However when carrier frequency $k \sim k_c$ need the TNLS (3rd order NLS).
- TNLS has no single-hump-envelope solutions.
- Analytical solution for single-hump-envelope wavepackets available if extra nonlinear terms added to give the HONLS (higher order NLS).

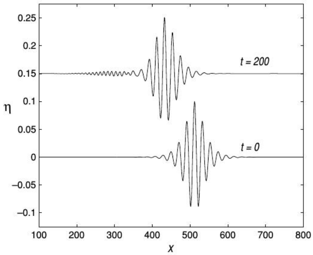

Figure 1. Numerical solution of the Ostrovsky equation for the initial condition of a wave packet given by (8, 11), at criticality $k = k_c$. Here $\lambda = \nu = 1$, $\gamma = 0.01$ and the wave packet initial amplitude is $a = 0.1$.

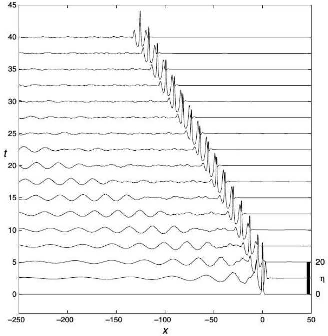

Coriolis platform: experiment

Grimshaw, Helfrich, J (2013)
Two-layers: Lower, salty 30cm. Upper fresh 6cm.
Box of fresh water (5m X 45cm) excess depth 3, 6, 9, 12 cm
Coriolis $f = 0, 0.105, 0.140, 0.209, 0.279\ \mathrm{s}^{-1}$

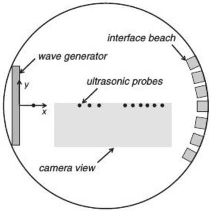

FIG. 10. Plan view sketch of the experimental set-up in the 13 m diameter Coriolis Platform.

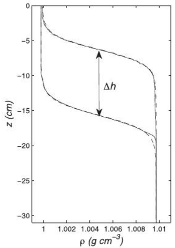

FIG. 11. Example of density profiles just prior to a rotating run inside (lower curve) and outside (upper curve) the reservoir. The dashed lines are best fits of (25). The measured reservoir depth Δh is indicated.

Coriolis platform: observations

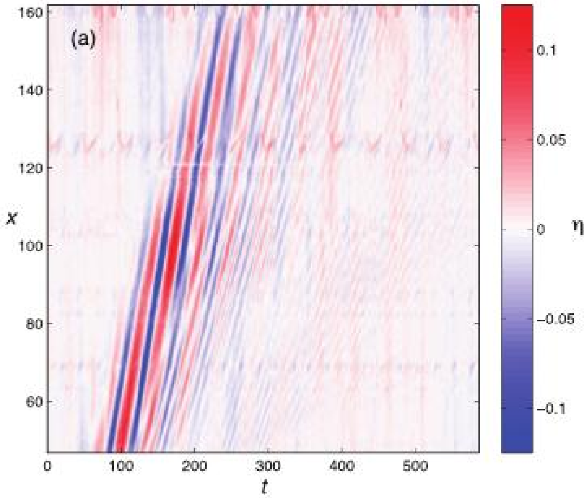

Interfacial displacement $\eta(x,t)$ along $y=-3.33$ from the overhead cameras.

Coriolis platform:
packet speed & carrier wavenumber comparisons

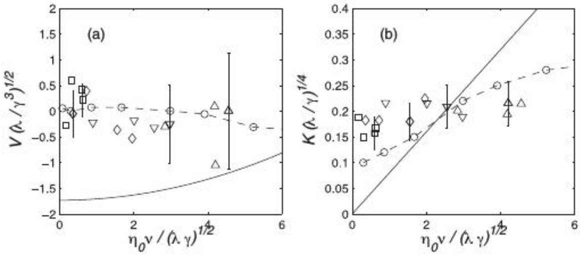

FIG. 23. (a) The nonlinear correction to the group speed V versus packet amplitude η_0. (b) The packet wavenumber K versus η_0. The results are non-dimensionalized using the scaling (17). The solid lines show the predictions from the NLS model. The circles with the connecting dashed lines show results from the numerical solutions of the Ostrovsky equation (6). The experimental results are indicated as $f = 0.098$ (triangle up), 0.131 (triangle down), 0.196 (diamond), and 0.262 (square).

The initial value problem: The TNLS model for the Gardner-Ostrovsky equation

TNLS for the Gardner-Ostrovsky equation

$$(\eta_t + \eta\eta_x + \nu\eta^2\eta_x + \eta_{xxx})_x = \eta.$$

- The additional cubic term leads to more accurate modelling of higher amplitude waves.
- The linear dynamics are the same as the Ostrovsky equation.
- Derive a TNLS valid for wavenumbers close to k_c (where ω_{0kk} vanishes) following GH08:

$$\mathrm{i}(A_t + c_g(k_c)A_x) - \mathrm{i}\frac{1}{6}\omega_{0kkk}A_{xxx} + \mu|A|^2A = 0.$$

The initial value problem for the Gardner-Ostrovsky equation

- The Gardner equation has soliton solutions of the form $\eta(x,t) = \eta_0(x-ct)$ where

$$\eta_0(x) = a_s/[b + (1-b)\cosh^2(x/D)].$$

- The leading order linear solution at large time to the GO equation with initial condition $\eta_0(x)$ is then the Airy wavetrain

$$\eta(x,t) \approx \frac{2\hat{\eta}_0(k_c)}{(12t)^{1/3}} \,\mathrm{Ai}\left(\frac{x - c_g(k_c)t}{(12t)^{1/3}}\right) \cos(k_c x - \omega_0(k_c)t),$$

where the amplitude $\hat{\eta}_0(k_c)$ is given by the Fourier transform of the initial condition at k_c, the zero-dispersion point.

The corresponding problem for the TNLS

The solution of the TNLS corresponding to the solution

$$\eta(x,t) \approx \frac{2\hat{\eta}_0(k_c)}{(12t)^{1/3}} \operatorname{Ai}\left(\frac{x - c_g(k_c)t}{(12t)^{1/3}}\right) \cos(k_c x - \omega_0(k_c)t),$$

of the GO is simply

$$A(x,t) \approx \frac{\hat{\eta}_0(k_c)}{(12t)^{1/3}} \operatorname{Ai}\left(\frac{x - c_g(k_c)t}{(12t)^{1/3}}\right),$$

precisely exact solution of the linear TNLS with initial condition

$$A(x,0) = \hat{\eta}_0(k_c)\delta(x).$$

The TNLS IC = energy at the zero-dispersion point in GO IC concentrated at the origin.

Ostrovsky/TNLS interface displacement comparison

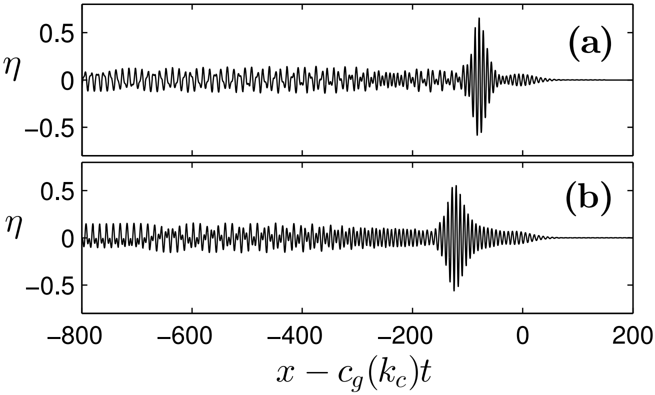

Interface displacements at $t = 1000$ from solutions of

- (a) the Ostrovsky equation with KdV IC with amplitude $a_s = 4$.
- (b) The TNLS with corresponding delta function IC

Ostrovsky/TNLS spectra comparison

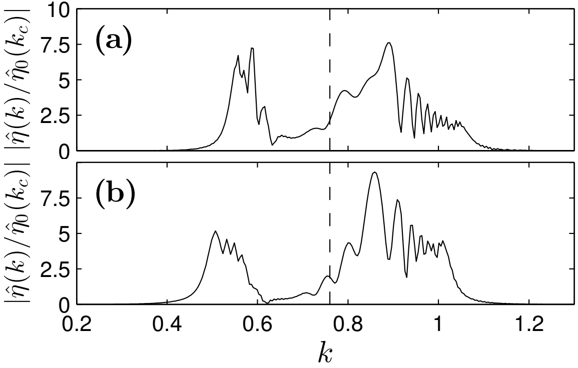

Wavenumber spectra at $t = 1000$ from solutions of

- (a) the Ostrovsky equation with KdV IC with amplitude $a_s = 4$.
- (b) The TNLS with corresponding delta function IC

The TNLS spectrum is translated by k_c with $k = k_c$ dashed.

Ostrovsky/TNLS wavenumber/amplitude comparisons

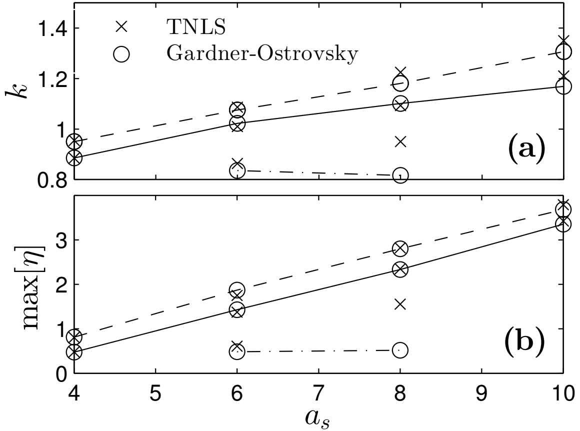

- (a) observed wavenumber k. (b) maximum amplitude
- ◯ Gardner-Ostrovsky $(\nu \neq 0)$; X TNLS.
- ——— $\nu = 0$; - - - - - - - $\nu = 0.1$; $- \cdot - \cdot - \cdot - \cdot$ $\nu = -0.1$.
- At time $t = 5000$.

GO integrations for opposite polarity ICs

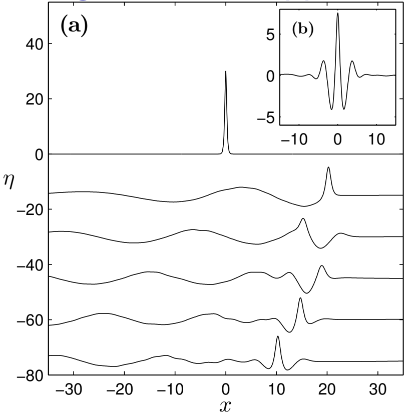

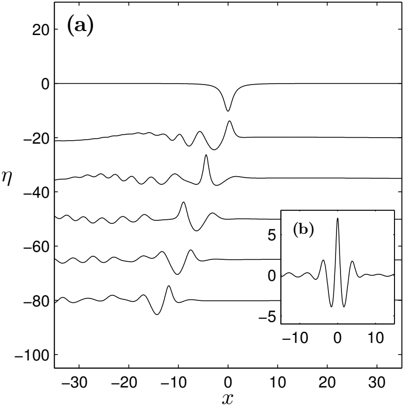

- (a) initial Gardner soliton ($\nu = 0.2$, $t = 0, 1, 2, 3, 4, 5$).
- (b) final packet ($t \approx 100$).
- Left: $a_s = 30$. Right: $a_s = -10.23$.
- Same value of $\hat{\eta}_0(k_c)$.
- Almost identical packet even though highly nonlinear.

The wavepackets in more detail

Wavepackets

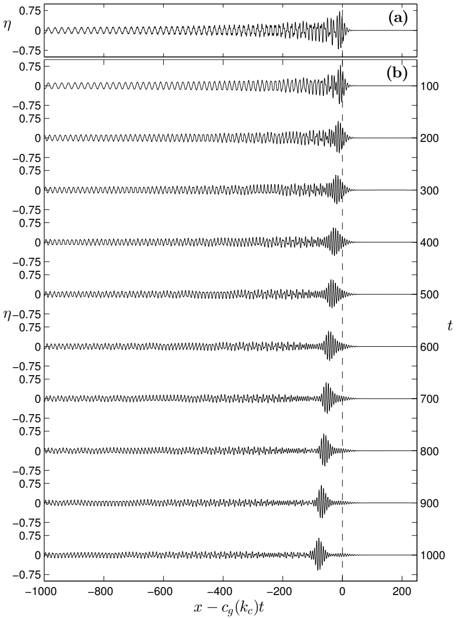

- Whitfield & J (2014): parameterless Ostrovsky with KdV IC.
- Only parameter the initial amplitude a_s. Here $a_s = 4$.
- Shown in frame moving at $c_g(k_c)$.
- (a) linear (b) nonlinear (little diff. at $t = 100$)
- Packet slightly slower than $c_g(k_c)$.

Wavepackets

$$F(s,T) = \int_0^L [\eta(x,0) - \eta(x - sT, T)]^2 \, \mathrm{d}x \Bigg/ \int_0^L \eta^2(x,0)\, \mathrm{d}x$$

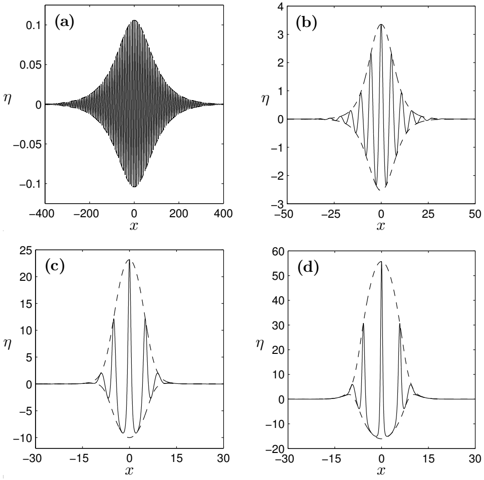

- Integrate until dispersive waves negligible.
- Use as IC to minimize F in (s, T) space.
- s group speed, T period.
- Less than 10^{-5}.
- Dashed curves – envelope
- (a,b) Near linear (c,d) Near KdV

Near-linear wavepackets, $A \ll 1$. Strong rotation

Near-linear wavepackets, $A \ll 1$. Strong rotation

- Follow GH08, expanding $\eta(x,t) = A_0 + A\exp(\mathrm{i}\theta) + \mathrm{c.c.} + A_2\exp(2\mathrm{i}\theta) + \mathrm{c.c.} + \ldots$.
- Fast phase $\theta = kx - \omega t$. k, undetermined carrier wavenumber.
- $A(x,t)$ slowly varying.
- $A_2 \sim \mathcal{O}(|A|^2)$.
- Then (GH08) $A_0 \sim \mathcal{O}(|A|^4)$. $[\gamma \sim \mathcal{O}(1)]$.
- A satisfies the usual second-order NLS, $(X = x - c_g t)$,

$$\mathrm{i}A_t + \frac{1}{2}\omega_{0kk}A_{XX} - \omega_2|A|^2A = 0.$$

- $\omega_{0kk} = c_g'(k)$ measures dispersion and is taken as non-zero as TNLS shows that energy is moved from $k = k_c$.
- $\omega_2 = \omega_2(k)$, measures nonlinear steepening.

NLS wavepackets, $A \ll 1$. Strong rotation

This has the finite-amplitude solution, correct to second-order in the amplitude,

$$\begin{aligned}\eta =& 2a\,\mathrm{sech}[K(x-c_g t)]\cos[k(x-c_c t)]\\ &+2a^2(\omega_2/k)\mathrm{sech}^2[K(x-c_g t)]\cos[2k(x-c_c t)]\\ &+\mathcal{O}(a^3).\end{aligned}$$

- $c_c = (\omega_0 + \frac{1}{2}a^2\omega_2)/k$ is the phase speed with nonlinear quadratic correction.
- The solution is not steady in any frame.
- The envelope is steady in a frame moving at speed c_g.

Computed wavepackets, $A \ll 1$. Strong rotation

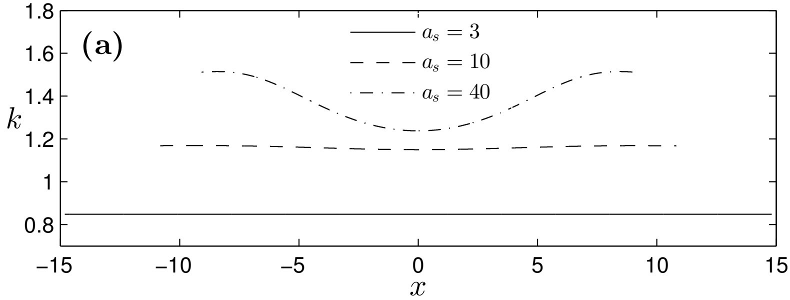

- Wavenumber k appears constant throughout packet for initial amplitudes up to $a_s = 10$.
- Thus NLS should be a good model up to $a_s = 10$.
- Use this measured k in the NLS soliton solution and choose amplitude a to give correct range.

NLS wave envelopes *versus* computed envelopes

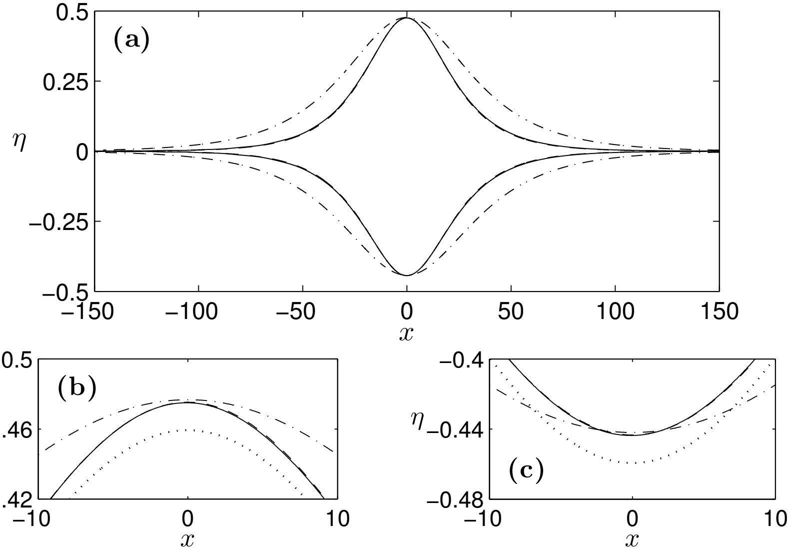

Solid: computed. Dashed(indistinguishable): 2nd order NLS.
Dotted: 1st order NLS. Dash-dotted: HO NLS

NLS wave speeds *versus* computed speeds

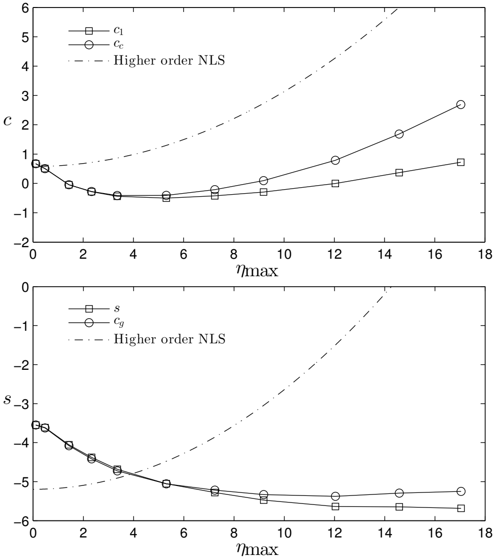

Crest speeds

- □ – c_1, measured phase speed at centre of packet.
- ○ – c_c, predicted phase speed with quadratic correction.

Envelope speed

- □ – s, measured group speed.
- ○ – c_g, predicted group speed.
- Using measured a, k

Near-KdV wavepackets, $A \gg 1$. Weak rotation

$A \gg 1$. The modulation equations

$$(u_t + uu_x + u_{xxx})_x = \pm\epsilon^2 u,$$

'+' normal; '-' anomalous (strong shear/ optical systems: Alias, Grimshaw & Khusnutdinova 2014; Obregon & Stepanyants, 1998)

$$u(x,t) = u_0(\theta, X, T) + \epsilon u_1(\theta, X, T) + \epsilon^2 u_2(\theta, X, T) + \cdots ,$$

where the fast θ and slow X and T are defined as

$$\theta = \epsilon^{-1}\Theta(X, T), \qquad X = \epsilon x, \qquad T = \epsilon t.$$

Local frequency $\omega(X, T)$, wavenumber $k(X, T)$ and phase velocity $c(X, T)$ are defined by

$$\omega = -\Theta_T, \qquad k = \Theta_X, \qquad \omega = kc,$$

and are related by the consistency condition,

$$k_T + (kc)_X = 0,$$

describing the conservation of waves.

The averaged equations

Removing secular terms at 2nd order by requiring orthogonality to adjoint of 1st order gives

$$\langle u \rangle_T + \frac{1}{2}\langle u^2 \rangle_X = \pm \partial_x^{-1} \langle u \rangle,$$
$$\frac{1}{2}\langle u^2 \rangle_T + \frac{1}{3}\langle u^3 \rangle_X - \frac{3}{2}(k^2 \langle u_\theta^2 \rangle)_X = \pm \langle u \partial_x^{-1} \langle u \rangle \rangle.$$

where the mean of any $2P$-periodic function $v(\theta)$ is defined as

$$\langle v \rangle = \frac{1}{2P} \int_{-P}^{P} v(\theta) \mathrm{d}\theta.$$

and for any $V(X)$,

$$\partial_x^{-1} V = -\int_X^L V(X') \mathrm{d}X' = \partial_x^{-1} \langle V \rangle.$$

Modulated cnoidal wavetrain

KdV cnoidal wavetrain satisfies zero order equation

$$u = a\{b + \mathrm{cn}^2[\beta(\theta - \theta_0)]\} + d,$$

with cn the Jacobi elliptic function with parameter m. Choose b so that d is the mean value of u, i.e. $d = \langle u \rangle$. This satisfies (integrating KdV twice)

$$k^2 u_\theta^2 = 2A + 2Bu + cu^2 - u^3/3, \qquad (2)$$

with $A = A(a, b, c, d, m)$, $B = B(a, b, c, d, m)$.

Modulated cnoidal wavetrain equations

Substituting into the averaged equations gives the governing system

$$k_T + (ck)_X = 0,$$
$$d_T + (cd + B)_X = \pm\partial_x^{-1} d,$$
$$(cd + B)_T + [c(cd + B) - A]_X = \pm(1/2)[(\partial_x^{-1} d)^2]_X.$$

Follow Whitham and introduce Riemann variables

$$r_1 = q + r, \quad r_2 = r + p, \quad r_3 = p + q,$$

where $p(a, d, m)$, $q(a, d, m)$, $r(a, d, m)$, $(r \leq q \leq p)$ are the three roots of the cubic on the right hand side of (2). The modulation equations become

$$r_{iT} + Q_i(r_1, r_2, r_3) r_{iX} = \pm 2(\partial_x^{-1} d), \quad \text{for} \quad i = 1, 2, 3,$$

where each r_i propagates with characteristic velocity Q_i.

Wavepacket solutions

For solutions steady in a frame moving at some speed s. Write $X' = X - sT$, $r_i = r_i'(X')$, $Q_i = Q_i'(X')$, $d = d'(X')$. Substituting and dropping dashes gives

$$\frac{\mathrm{d}r_i}{\mathrm{d}X} = \pm\frac{2D}{(Q_i - s)}, \quad \text{normal/anomalous}$$

where $\mathrm{d}D/\mathrm{d}X = d$.

These odes were integrated numerically away from $X = 0$.

Wavepackets with anomolous dispersion - Ostrovsky -

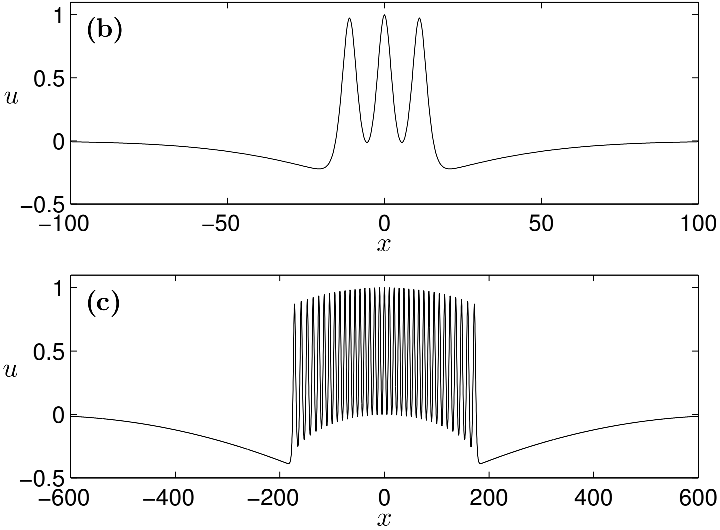

(b) A 3-peak packet solution with $\epsilon = 0.0207$ and $c_0 = 0.138$.

(c) A 35-peak packet solution with $\epsilon = 0.00320$ and $c_0 = 0.0213$.

The modulation equation solution for (c) above

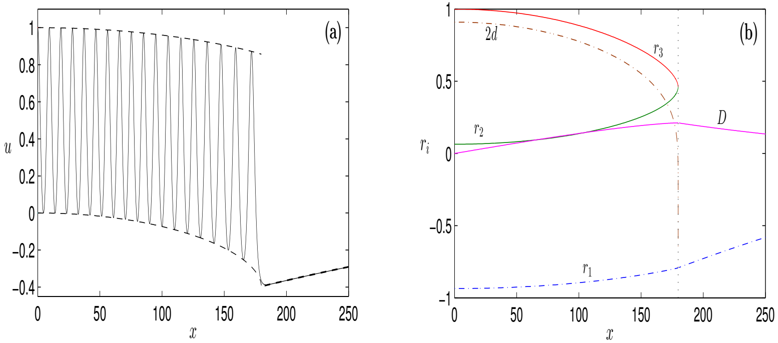

(b) The Riemann variables: r_1 (dash-dot blue), r_2 (dashed green), r_3 (solid red); D (solid magenta) and $2d$ (dash-dot brown). The vertical dotted line ($x \approx 180$) gives the point where the numerical solution terminates.

Modulation solution for normal dispersion -unsteady packet-

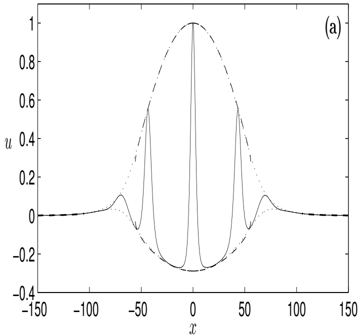

(a) Dotted lines: numerically determined envelope. Dashed lines: modulation solution.
(b) The Riemann variables
Here $\epsilon = 0.018$.

Modulation solution for normal dispersion
-periodic wavetrain-

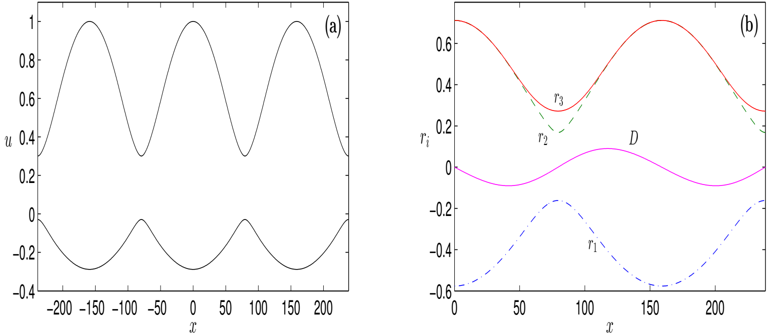

Here $\epsilon = 0.018$.

Conclusions

- Wavepacket formation is sufficiently well captured by the TNLS to give accurate predictions of packet amplitudes and carrier wavenumber (determined by $\hat{\eta}(k_c)$).
- The ZDP divides the spectrum of the GO into modulationally stable and modulationally unstable regions and nonlinearity moves energy into these regions away from k_c.
- The energy moving to the focussing region forms the wavepacket described by the second order NLS.
- There are two distinct regimes: strong rotation and large amplitude.
- In the strong rotation regime a second-order NLS solution reproduces the shape, group speed and phase speed of the near-linear packets.
- In the large amplitude regime Whitham modulation equations describe the near-KdV packets, both for normal and anomalous dispersion.

Modulational instability, MI

- It appears that wavepackets in strong rotation are NLS solitons.
- Can we predict k and a?
- One possibility is modulational instability (MI).
- Lighthill (1965):
  - Dispersion relation with frequency correction quadratic in amplitude (as here).
  - Infinite wavetrain is unstable to MI, Benjamin-Feir instability, if $\omega_{0kk}\omega_2 < 0$.
  - Never for KdV. Always for $k > k_c$ for Ostrovsky.
  - The modulation wavenumber must satisfy $0 < K < K_c$ where $K_c = a\left(-4\omega_2/\omega_{0kk}\right)^{1/2}$.

Ostrovsky group velocity

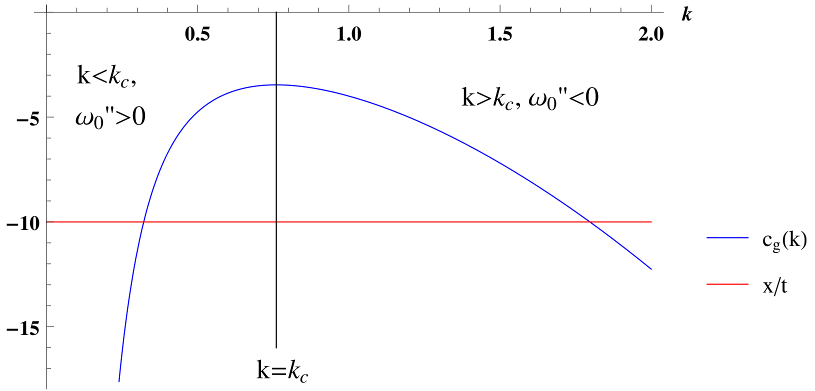

Localised Gaussian modulations

Finite wavetrain example. Both carriers have $k = 0.9 > k_c$ thus satisfy BFL for MI, i.e. focussing.
Estimate a local $K = \frac{1}{A}\frac{\mathrm{d}A}{\mathrm{d}x}$.
Dashed lines show modulation envelope at $t = 0$.

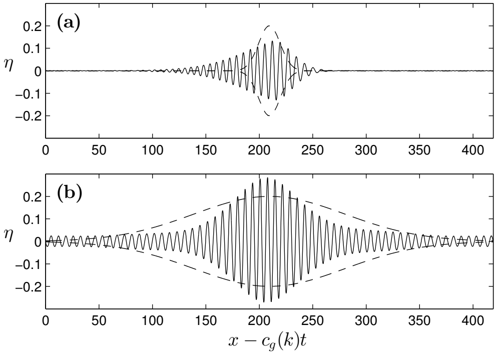

- (a) Stable modulation at $t = 100$ with large K ($K = 0.07$). Spreads through linear dispersion.
- (b) Unstable modulation at $t = 1,500$ with small K ($K = 0.01$). Grows through nonlinearity.

Ostrovsky group velocity: stationary phase

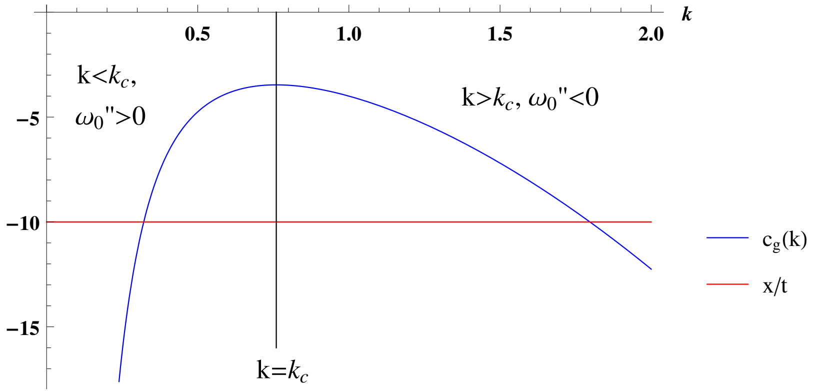

Stationary phase for KdV IC

For wavenumbers away from k_c, this gives the leading order behaviour as the sum of two slowly varying linear wavetrains,

$$\eta(x,t) \approx \eta_+ + \eta_-, \quad t \to \infty,$$

with wavenumbers $k_- < k_c < k_+$,

$$k_\pm(x,t) = 6^{-1/2}\left\{-(x/t) \pm \left[(x/t)^2 - 12\right]^{1/2}\right\}^{1/2}$$

and amplitudes

$$\eta_+ = 2A_+ \cos(k_+ x - \omega_0(k_+)t + \pi/4), \quad A_+ = \hat{\eta}_0(k_+)[2\pi|c_g'(k_+)|t]^{-1/2},$$

and

$$\eta_- = 2A_- \cos(k_- x - \omega_0(k_-)t - \pi/4), \quad A_- = \hat{\eta}_0(k_-)[2\pi|c_g'(k_-)|t]^{-1/2}.$$

Modulational constraint

$0 < K < K_c$ becomes $K^2 < -4a^2\omega_2/\omega_{0kk}$,
i.e. $B(x,t) < 4$, where

$$B(x,t) = -(K^2/a^2)\frac{\omega_{0kk}}{\omega_2} = -\frac{1}{A_+^4}\left(\frac{\mathrm{d}A_+}{\mathrm{d}x}\right)^2\frac{\omega_{0kk}}{\omega_2}.$$

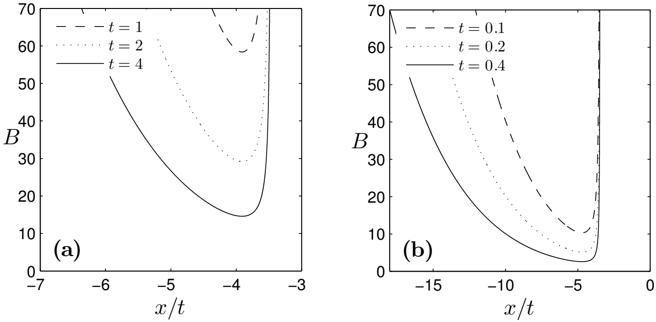

- Initial KdV soliton amplitudes (a) $a_s = 3$. (b) $a_s = 10$.
- Instability occurs at larger t for smaller initial amplitude solitary waves (GH08).
- $x/t = c_g(k_B)$ determines local wavenumber, k_B.

Predicted k_B, $--$, versus measured k_3, $\circ$.

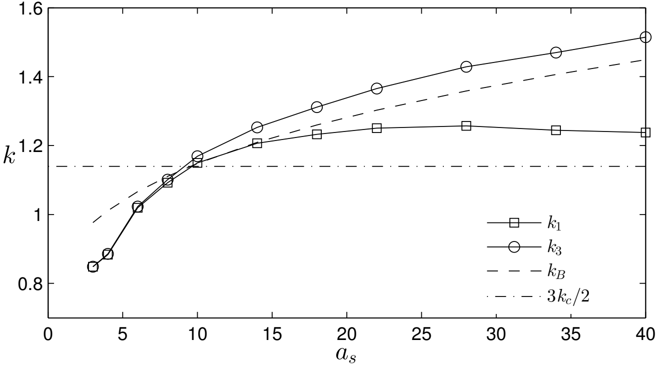

Solid: measured. k_3 at packets edges, $\circ$.

Dashed: predicted k_B, $--$.

Conclusions

- Packet solitons have been found in a laboratory experiment. In the oceans the main supporting evidence is that some soliton wavetrains appear to be not rank-ordered.
- It is possible to construct numerically highly accurate packet solutions of the Ostrovsky equation.
- There are two distinct regimes: near-linear and near-KdV.
- In the near-KdV regime the GHO generation mechanism seems relevant.
- In the near-linear regime a second-order NLS solution reproduces the shape, group speed and phase speed of the packets.
- Modulational instability of a linearly dispersed wavetrain gives a good approximation for the carrier wavenumber of near-linear packets and offers a possible explanation of why packets can appear even when they do not separate from the dispersive wavetrain.